Astron. Astrophys. 319, 331–339 (1997)

ASTRONOMY
AND
ASTROPHYSICS

Laser induced fluorescence spectroscopy of jet-cooled molecular species: a tool to identify diffuse interstellar band carriers

C. Moutou[1], **L. Verstraete**[1], **P. Bréchignac**[2], **S. Piccirillo**[3], **and A. Léger**[1]

[1] Institut d'Astrophysique Spatiale, CNRS Université Paris Sud, Bâtiment 121, F-91405 Orsay, France
[2] Laboratoire de Photophysique Moléculaire Université Paris Sud, Bâtiment 213, F-91405 Orsay, France
[3] C.N.R Istituto Materiali Speciali, Tito Scalo (PZ), Italy

Received 30 April 1996 / Accepted 30 July 1996

Abstract. We present the first results of an experimental method (jet expansion followed by laser induced fluorescence) that collects absorption spectra of cold, gas-phase isolated species. This method, closely simulating interstellar conditions, is a powerful tool to assert diffuse interstellar bands (DIB) identification. It only requires the species studied to be fluorescent. This latter condition is fulfilled for some DIB carriers as shown recently. Stimulated by the recent detection in rare-gas matrices of its fluorescence, we focus on the perylene cation. This molecule pertains to a family (the polycyclic aromatic hydrocarbons or PAHs) whose ions or radicals are potential DIB carriers. We failed to detect the fluorescence observed in rare-gas matrix. Rather, we observed a photofragmentation process leading to the C_2 molecule. We thus obtained the absorption spectrum of a PAH radical of size comparable to its parent molecule, perylene. From a comparison with the DIB spectrum, we find that rotationally broadened bands of PAH radicals may explain the profile of broad DIBs, or regularly spaced DIBs sequences.

Key words: ISM: dust; molecules – methods: laboratory – molecular processes

1. Introduction

Since the turn of the century, up to 200 diffuse interstellar bands (DIBs) have now been observed (Jenniskens & Désert 1994) in absorption against many lines of sight and the question of their identification is still opened (Herbig 1995). There is now strong evidence that the carriers are large, carbon-bearing species absorbing in the visible/near-IR range (Scarrott et al. 1992, Herbig 1995, Sarre et al. 1995). In addition, in the conditions prevailing in the interstellar medium (ISM), DIB carriers are cold and isolated (i.e., gas phase species). A firm DIB assignment can therefore only be achieved from comparison of astronomical and laboratory data when the latter have been obtained in (or can safely be extrapolated to) conditions close to interstellar.

Some gas-phase experiments have been done on species produced by vaporization of a solid sample (Flinckinger et al. 1991, Kurtz 1992) but the molecules so produced are hot and suffer mutual collisions. To date, the technique simulating best the interstellar environment locks up the sample molecule in a rare-gas matrix whereby it is cold (a few K) and isolated from its companions (Salama and Allamandola 1992, Léger et al. 1995). However, the sample molecule always interacts, although very weakly (as in neon matrices), with the rare-gas substrate and absorption lines are broadened and displaced towards the red (by a few tens of Å). Unfortunately, the effect of the matrix depends specifically on the substrate/sample molecule interaction and no quantitative extrapolation can be drawn from the results on the few species for which both matrix and gas-phase spectra exist (Léger et al. 1995). This effect is even larger in the case of ions. Therefore, only rough guesses can be performed which do not lead to positive DIB identifications. In addition, in contrast with the ISM, the matrix blocks any rotation motion of the molecule: this quenching may substantially change the absorption profiles peculiarly for large molecules. Hence, the match (or mismatch) of a matrix spectrum with astronomical data may be indicative but inconclusive.

We have designed an experiment aimed at collecting absorption spectra of cold molecules in the gas phase using the laser induced fluorescence (LIF) signal. This technique requires the molecule under study to be fluorescent. Our approach has been stimulated by recent observations of red emission counterparts to 7 DIBs (Rao & Lambert 1993, Scarrott et al. 1992) demonstrating that some DIB carriers are indeed fluorescent species.

We set out to study a polycyclic aromatic hydrocarbon (PAH) named perylene in its cationic form ($C_{20}H_{12}^+$). This choice has been motivated by a recent laboratory study in rare-gas matrix bearing out evidence of the fluorescence of the perylene cation (Joblin et al. 1995).

Although the perylene cation has not been claimed to be at the origin of any DIB, PAH ions and radicals are amongst good

Send offprint requests to: C. Moutou

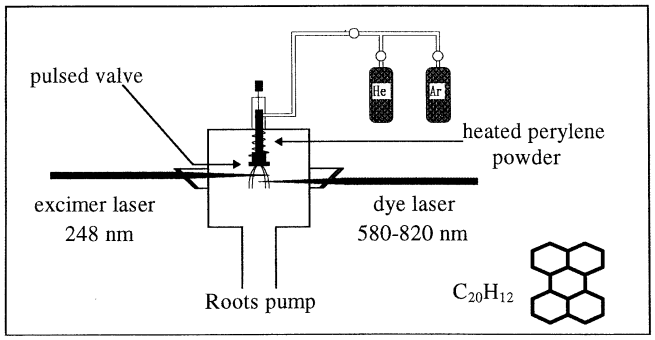

Fig. 1. A partial sketch of our experimental set-up. The pulsed jet supersonically expands into the vacuum chamber after mixing of the sample molecules with helium or argon carrier gas. It is first crossed with the excimer laser beam and, 1 cm downstream, with the dye laser one. The fluorescence signal induced by the dye laser is collected by a lens whose axis is perpendicular to the laser beams. It is then dispersed by monochromators and sent onto a photomultiplier or a CCD array.

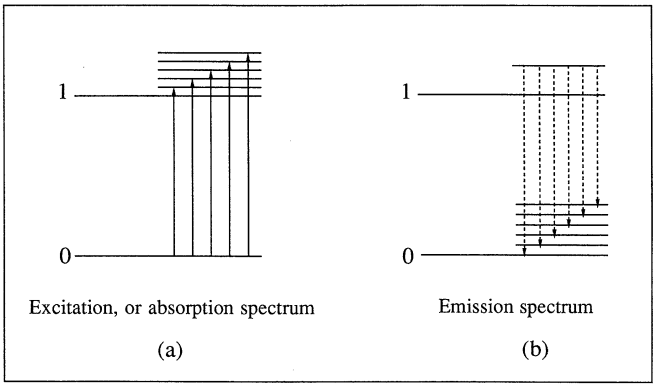

Fig. 2a and b. The meaning of LIF spectrocopy is outlined. **a** The excited state of the emitting species is probed when the total fluorescence signal (monochromator's slits widely opened) is sent to the photomultiplier (excitation, or absorption, spectrum). **b** Conversely, the species' ground state is probed while the fluorescence is dispersed in the monochromator (emission spectrum).

candidates for DIB carriers (Léger 1994, Herbig 1995). Since the original proposal that PAH cations may produce some DIBs (van der Zwet & Allamandola 1985, Léger & d'Hendecourt 1985, Crawford et al. 1985), a large number of absorption studies of small (containing up to 32 carbon atoms) PAHs cations in rare-gas matrices has been accumulated (Salama & Allamandola 1992, 1993; Ehrenfreund et al. 1992). Undeniably, PAH cations absorption profiles could match the strongest DIBs (Léger, 1994). The presumption in favor of PAH cations has been reinforced by recent transition energy quantum chemistry calculations (Parisel et al. 1992). Encouraging DIB assignments with the pyrene cation and its derivatives (Salama & Allamandola 1993; Léger et al. 1995) have been recently proposed on the basis of matrix spectra. In a similar context, two near-IR DIBs have been attributed to C_{60}^+ (Foing & Ehrenfreund 1994).

To confirm these attributions, gas-phase spectra of cold molecules are needed. It must be stressed, however, that rare-gas matrices experiments, routinely conducted over a wide spectral range, are essential to usefully guide LIF studies.

2. Experimental method

Our experimental set-up is sketched on Fig. 1. It is a modified version of that described in Moreels et al. (1994). The sample molecules are born by a molecular jet which is intersected with two parallel laser beams in opposite directions. The first laser ionizes (and/or fragments) the parent molecules and the second one probes the products for induced fluorescence after an appropriate time delay. We operate in a chamber with pressure of about 0.1 mbar. The gas in the jet is a mixture of an atomic carrier gas (helium or argon) and of PAHs vaporized from a powder sample. The backing pressure of the carrier gas is high (up to 5 bars); it is supersonically expanded in the low pressure chamber by passing through a heated nozzle of diameter 0.5 mm. The nozzle is closed by a valve pulsed at a frequency of 15 Hz and kept opened during ca 2 ms.

The density in the jet rapidly decreases after the nozzle as the square of the distance to the nozzle. The jet is first crossed with the focussed ($\sim$ 1mm spot size) beam of an excimer laser close to the nozzle (a couple of mm below) to maximize excitation efficiency. The excimer laser pulsed at a repetition rate of 15 Hz, delivers a radiant energy of ca 150 mJ in each pulse of 15 ns duration. As neutral perylene exhibits a strong absorption band at 250 nm (the β-band, see Clar 1964), we selected a gas mixture to get the KrF excimer emission at 248 nm. The ionization potential (IP) of perylene being 7 eV (Leach 1987), two 248 nm-photons sequentially absorbed can ionize perylene.

The products of this first interaction then travel 1 cm downstream before encountering the beam of a Quantel dye laser, pumped by a Nd^{3+}:YAG laser, whose wavelength is tunable from 560 to 750 nm and extended to $\sim 1\ \mu m$ by stimulated Raman scattering in a high pressure H_2 cell (see Bréchignac et al. 1986). The dye laser is triggered at 15 Hz and with the adequate time delay to ensure coincidence of the species earlier hit by the excimer laser. The delay depends on the carrier gas mass, it is of the order of 5 μsec in helium and 15 μsec in argon. The pulsed valve is synchronized with the laser pulses.

On their pathway through the 2 laser excitations, molecules are cooled very efficiently by collisions with the carrier gas. Possibly formed electronically excited states will also radiate to the electronic ground state during this delay. Typical rotation (vibration) temperatures currently achieved in such supersonic jets are 1–10 K (20–100 K). Moreover, the jet is very nearly monocinetic with a translational temperature down to 1 K so that there are no mutual collisions between molecules at the probing laser location. Argon has been recognized to be a more efficient jet coolant than helium (Smith et al. 1987 and this experiment): we therefore used it as carrier gas. In argon, however, clusters form

more easily than in helium. We checked for the presence of van der Waals clusters by comparing excitation spectra (see below) obtained with helium and argon as carrier gases. As we found no significant spectral changes, we are confident that our results are not contaminated by the presence of clusters. Indeed, even if such weakly-bound species were formed in small concentration they would have almost no chance to survive after absorption of two (or more) 5 eV photons.
The supersonic jet producing cold and isolated molecules represents a very close simulation of interstellar conditions. Another advantage of the free jet is that the cations or radicals produced have little chance to recombine in the vacuum chamber where the density is decreasing very sharply away from the nozzle. Again, in contrast to rare-gas matrices where loosely trapped electrons and small fragments can diffuse to recombine, we can preserve most ions and radicals produced in the jet.

Collecting on the detector the fluorescence of the species excited by the dye laser, two kinds of measurements can be made. Monitoring the fluorescence signal while scanning the dye laser frequency provides an excitation spectrum, that gives the structure of the excited state (Fig. 2a): indeed, assuming a constant fluorescence quantum yield as a function of excitation wavelength, the excitation spectrum is expected to be proportional to the absotpyion spectrum. We can also, at fixed laser excitation wavelength, disperse the fluorescence and obtain an emission spectrum, which provides the ground state structure of the emitter(Fig. 2b).

The laser induced fluorescence photons go through a lens whose axis is perpendicular to the laser beams to reach the entrance slit of a monochromator. Two apparatus are then available to detect the signal. The first one is well-suited for absorption spectroscopy: we use a Jobin-Yvon monochromator with 1200 grooves mm^{-1} and wide entrance slit ($\sim$ 1 mm). It is dispersive enough, however, to reject scattered laser light. At the exit slit the photons are collected on a Hamamatsu R943–02 photomultiplier. The signal is then gate-processed by a Boxcar integrator after proper amplification, and averaged over a selectable number (10 to 50) of laser shots before entering the data acquisition system. The gate is chosen so that the residual scattered light and eventual electronic noise are rejected. We obtain the structure of the absorbing species excited state. The laser linewidth is typically 0.1 cm^{-1}.

The second channel of detection is available for acquiring emission spectra. It is a second monochromator with two gratings of low and high resolution. The size of the entrance slit is tunable down to 25 μm, and its image is formed on a CCD chip 256*1024 pixels. This allows, when the excitation wavelength is fixed, to measure in one exposure the whole emitted spectrum with the lowest resolution grating (150 grooves.mm^{-1}), or to resolve one emission band with the 1200 grooves.mm^{-1} grating and a narrow slit. The highest resolving power obtained with this apparatus is $\sim$ 3000. The CCD image is transfered to a PC computer, where the spectrum is averaged over the chip height (256 elements), which increases the S/N ratio. This detection is dedicated to probe the structure of the fluorescent species ground state, and therefore offers spectroscopical information complementary to the first channel described above.

To validate our experiment, we first studied the furan molecule photoexcited at 193 nm (ArF band) and reproduced quite well existing results (Smith et al. 1987). This experiment, contrarily to what was first announced, involved a neutral species (the C_3 radical) as the fluorescence carrier as has been realized later on (Smith et al. 1988). We used this test case to optimize the adjustments of the whole set-up.
We also reproduced the results obtained on neutral perylene in free jet (Schwartz and Topp 1984).

3. Search for the fluorescence of $C_{20}H_{12}^+$

Encouraged by the recent results of Joblin et al. (1995) in rare-gas matrices, we have looked for the fluorescence of the perylene cation using the LIF technique. The absorption spectrum of the perylene cation in a neon matrix shows two main bands near 525 and 730 nm. In matrices, the fluorescence signal is detected at longer wavelengths mostly in two bands near 790 and 810 nm. We tuned the dye laser on the 730 nm-band and thoroughly searched for fluorescence in a large domain (50 nm wide) centered at 800 nm but failed to observe the signal reported by Joblin et al. (1995).

The reasons of this non-detection may be:
(i) the excimer excitation forms few cations or perylene cations recombine efficiently, leaving preferentially neutral fragments,
(ii) the fluorescence quantum yield of the perylene cation in the gas phase is much lower than in matrices,
(iii) the emission observed by Joblin et al. (1995) is phosphorescence rather than fluorescence while our experiment acquiring signal on short timescales (a few μsec) is weakly sensitive to phosphorescence.
(iv) the species emitting in the matrix (Joblin et al. 1995) is not the perylene cation and this alternate species is pumped by energy transfer.

We do not have material to sort within these possibilities. Nonetheless we think that (ii) is more probable and (iv) is less probable.

4. Results

4.1. Absorption spectrum of a perylene fragment

Looking for perylene cation fluorescence in our experiment, we found an unexpected signal towards the blue of the absorption wavelength. It could be explained either by multiple absorption of visible photons or by photoinduced fragmentation. To answer this question, we examined the laser energy dependence of this signal. The relationships between the fluorescence intensity and the intensities of both laser beams are plotted in Fig. 3. They show that four 248 nm-photons are absorbed, while only one dye-laser photon (slopes $\sim$ 4 and $\sim$ 1 respectively). This last

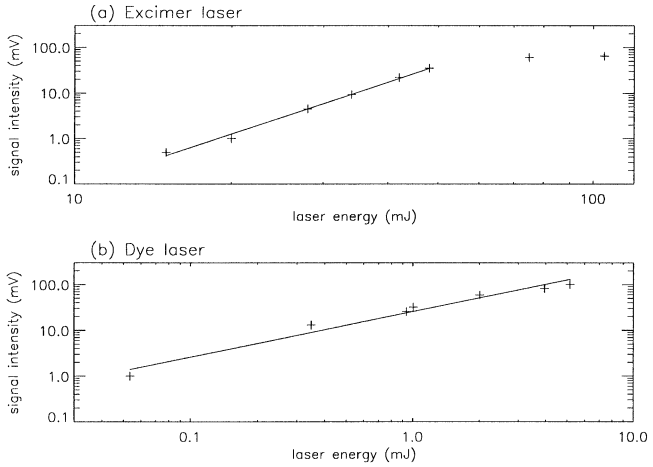

Fig. 3a and b. Relationships between the total fluorescence signal and **a** the excimer laser intensity, **b** the dye laser intensity at λ= 6290.7 nm. The best fit lines have slopes of 3.96 and 0.89 respectively. Saturation can be seen in panel (**a**). Similar relationship was found for any resonant wavelength of the dye laser.

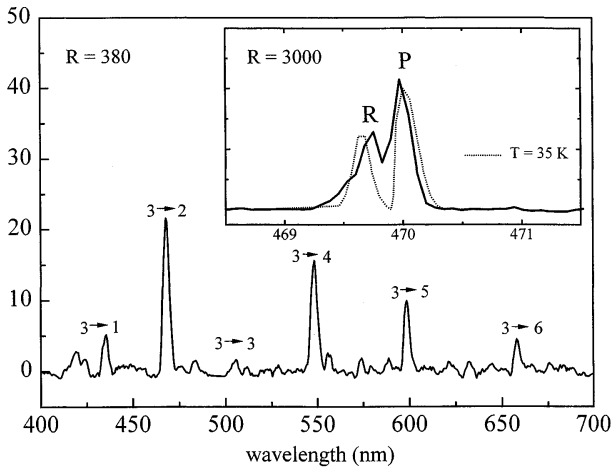

Fig. 4. The emission spectrum of C_2, after excitation of the X species at 721.7 nm. A Swan bands series is observed, with bands at 437, 470, 505, 550, 600 and 660 nm. In the inserted frame we show a spectrum taken at higher resolution (R $\sim$ 3000) of the strongest band (v'=3 to v"=2) at 470 nm, exhibiting the P and R rotational branches. Also shown in this frame is a simulation (see text) of the P and R branches (Q–lines neglected) at a rotational temperature of 35 K.

result implies that the emitting species is different from the one which absorbs the dye laser. We conclude that a fragmentation is induced by absorption of the dye laser photon, leading to a fluorescent product which emits at wavelengths shorter than absorption wavelengths. This emission was then spectrally analyzed in an attempt to identify the fluorescent product. The emission spectrum obtained for an excitation at 721.7 nm is displayed in Fig. 4. The fluorescent emission of the C_2 molecule in the well-known Swan bands series: $(d, v' = 3) \rightarrow (a, v" = 1 \text{ to } 7)$ at wavelengths $\sim$ 437, 470, 506, 550, 600, 660 nm can be easily recognized (see 4.2 below).

We then attempted to check for the ionic character of the species responsible for the absorption. Application of an electric field as high as 50 V cm^{-1} was found to have no effect on the fluorescence signal. The obvious conclusion is that the parent molecules of the emitting C_2 is a neutral species that cannot be identified at present stage, and we label X in the following.

The LIF excitation (absorption) spectrum of the X-species is shown in Figs. 5 & 6. It extends over the range 11,000–17,000 cm^{-1} (588–910 nm). The resolution of the tunable dye laser is of the order of 0.1 cm^{-1}. This spectrum is characterized by several groups of bands separated by a few 100 cm^{-1} typically. Each group is divided into a set of bands which are about 1 cm^{-1} wide, and separated by a few 10 cm^{-1}. The extension of a group is 50 to 80 cm^{-1}. We found the pattern of these spectral features to be insensitive to the laser intensities spanned in our experiments (see Fig. 3). We understand this spectrum as a progression of vibronic bands whose origin lies at 12,134.7 cm^{-1} (824.0 nm). The wavenumbers of active vibrational modes can thus be found from the distances to the origin. The widths of the bands within a group are compatible with rotational broadening of a large species. The multiplicity of each vibrational group of bands is probably due to electronic fine structure. There are 2 additional features towards the red of the origin which we believe are hot bands. We have tested this interpretation by trying to change the efficiency of collisional cooling in the jet. First, rising the backing pressure of the carrier gas increases the cooling of sample molecules. Second, for what regards the carrier gas, argon is a better coolant than helium as already mentioned (Sect. 2). Consistently with the hot band hypothesis, we observed that increasing the backing pressure and using argon in the jet resulted in weaker bands at 11,488 and 11,823 cm^{-1}.
The small widths of individual vibronic bands (1 cm^{-1} and less) correspond to a rotational temperature of a few K (Cossart-Magos & Leach 1990), as well as the weak intensity of the hot bands demonstrates that the X-species vibrational modes are efficiently cooled by collisions with the carrier gas between the excimer and dye laser excitations.
The strong $*$-band starting at 15,835 cm^{-1} may be the origin of a new electronic transition.

The third column of Table 1 gives the wavenumbers, taken from the origin, of the vibrational frequencies extracted from the excitation spectrum. Also given are the vibrational modes for neutral perylene (first column) and perylene cation (second column) that were found to match the X frequencies within about 50 cm^{-1}. It is remarkable that 9 modes among 15 of the X-spectrum are also present in $C_{20}H_{12}$ and/or $C_{20}H_{12}^{+}$. At frequencies larger than 2000 cm^{-1} the lack of measurements in the literature did not allow us any more comparison. In particular, the low-frequency butterfly mode of neutral perylene at 94 cm^{-1} is also present in the X-spectrum. From this we infer that the X-species must have an overall structure close to that of perylene, i.e., X is probably a large perylene fragment, possibly a partially dehydrogenated perylene. This is coherent with the re-

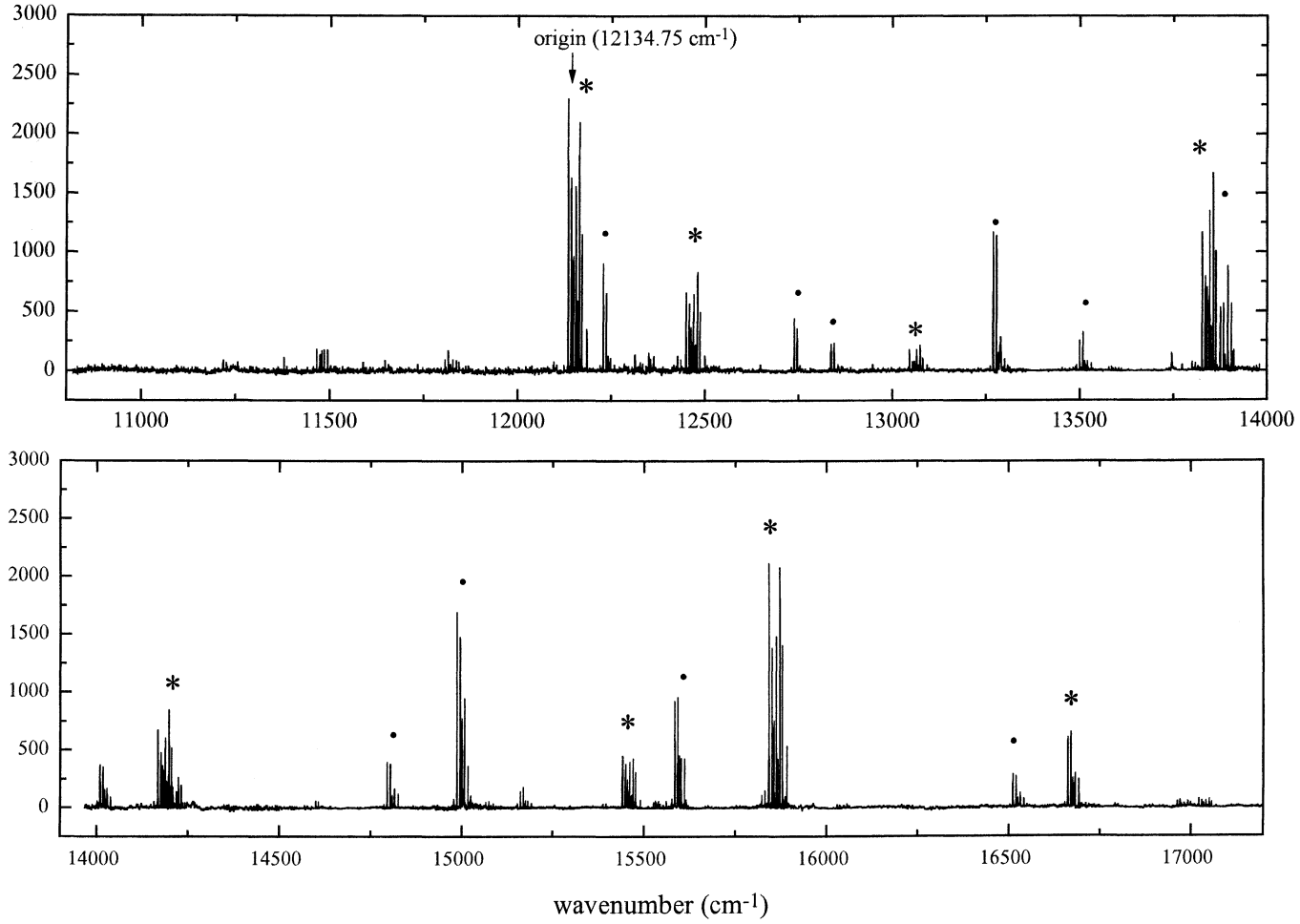

Fig. 5. Excitation (or absorption, see Sect. 2) spectrum of the X-species. It was recorded by measuring the whole fluorescence of C_2 in the strong 470 nm Swan band, as a function of the dye laser wavelength. The resolution of the dye laser is 0.1 cm^{-1}. 7 different dye solutions, and frequency shift by stimulated Raman scattering in H_2 have been necessary to cover this wide region (588–910 nm). We assign the main origin at 12,134.7 cm^{-1}. Another one is probably seen at 15,835 cm^{-1}. Two different groups of vibronic bands are labeled by $*$ and • (see Sect. 4.1).

sult of photofragmentation experiments (Jochims et al., 1994, P. Boissel, private communication): perylene preferentially ejects a H_2 fragment after a 18 eV irradiation; this result observed for cations should also be valuable for neutral species.

Fig. 6 shows an enlarged view of the excitation spectrum near the origin. Two different types of vibronic bands are distinguishable: (i) the origin itself, composed of 8 strong lines and (ii) the first vibronic band whose structure is much simpler with only 6 lines, and 2 major ones. All vibronic bands can be cast into these two different groups, which we label respectively $*$-bands (bands alike the origin) and •-bands (bands alike the first vibronic transition) (see Fig. 5). Fine structure intervals in each family vary slightly from one vibrational state to another as may occur in spectra of complex molecules where the density of states is high. We report in Table 2 the measured intervals, $\Delta\nu_i$, taken from the origin of each vibronic band (see Fig. 6). As can be seen, all the lines of the •-bands are present in $*$-bands with the exception of $\Delta\nu_2$. On the other hand, the $\Delta\nu_5$, $\Delta\nu_7$ and $\Delta\nu_8$-lines of $*$-bands are absent from the •-ones. Fine structure intervals are very similar (with a mere 10% deviation) in each band-class over 5,000 cm^{-1}.

We determined the temperature of the X-species in the jet with the code of Birss and Ramsay (1984), which computes the rotational spectrum of an asymmetric rotor. We used the exact values of perylene rotational constants, assuming a similar geometry for the X radical. The profiles are more symmetrical when the transition moment is taken in the plane formed by a and b axis. The measured widths in the spectrum (Fig. 6) are of the order 0.8–1 cm^{-1}, corresponding to a rotational temperature in the jet of 3–4 K. The species are thus very efficiently cooled.

4.2. C_2 emission

Fig. 4 presents the emission spectrum observed when exciting the X-species at 721.7 nm. The main spectrum shows some features at positions close to 437, 470, 505, 550, 600, and 660 nm. These emission bands are independent of the excitation wave-

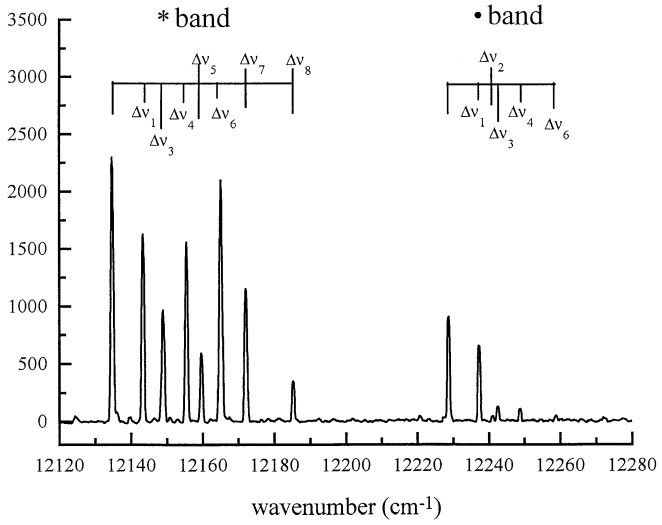

Fig. 6. Blown-up view of the first 2 vibronic bands representative of $*$ and •-type respectively. Frequency spacings of the characteristic features of the pattern are labeled as $\Delta\nu_i$, their values are listed in Table 2.

length, from 824 up to 585 nm. We identified these bands to the Swan band series of the C_2 molecule (Danylewych and Nicholls, 1974). Indeed, positions and intensity ratios are coherent with the initial vibrational level being $v' = 3$. A very selective excitation of C_2 occurs, that leaves the fragment in the $d^3\Pi_g, v' = 3$ state. Furthermore, our lifetime measurements from a digital oscilloscope (125 ± 10 ns) are also consistent with litterature data (Naulin et al. 1988).

The frame inserted in Fig. 4 shows the strongest 470 nm band at higher resolution ($\delta\lambda = 0.15$ nm). A substructure with two bands is visible, which we interpret as rotational P and R branches. The Q branch is too faint to be seen. We model this rotational contour, using molecular constants of Dhumwad et al. (1981), and find a rotational temperature of ~ 35 K to fit the observed width and intensity ratio between P and R branches. The small C_2 fragment is thus ejected with a relatively small rotational energy. This is consistent with a statistical unimolecular decay process. However, the origin of the selective vibrational excitation is unknown.

4.3. Fragmentation process

In this section, we outline the energetics and characteristic time constants involved in the formation of the X-species.

As discussed in Sect. 4.1, the parent molecule, perylene, sequentially absorbs 4 excimer photons at 248 nm in the sequence of processes leading to some species which fragments by absorption of visible light. The first absorption corresponds to a $S_0 \rightarrow S_3$-transition (or β-band, Birks 1970). Assuming an average absorption cross-section of 1.10^{-16} cm^{-2} (Joblin et al. 1992), it can be estimated that perylene absorbs a 5 eV-photon every 40 ps in the excimer beam. After the first 5 eV-excitation, perylene can relax only via fluorescent and/or vibrational cascades which both have longer timescales: a few nanoseconds at least and a few tenth of seconds, respectively (Léger et al. 1989b and references in Jochims et al. 1994). Indeed, no photofragmentation takes place in a short timescale in PAHs for internal energies below ~ 7 eV (Ling and Lifshitz 1995, Jochims et al. 1994 and Gotkis et al. 1993). The second 5 eV-photon thus excites the molecule at 10 eV above ground level. At such excitation energy, ionization and/or fragmentation processes can proceed efficiently. They will lead to either a radical R* or an ion I* (see Fig. 7) bearing at most an excitation energy of a few eV. This species will in turn, just as earlier, absorb sequentially two 5 eV-photons and give rise to a new species. If the intermediate is an ion I*, it will necessarily fragment since the loss of a second electron costs too much energy: the resulting heavy fragment would of course keep the charge. Should the intermediate be a neutral R*, it may ionize or fragment into X*. Since the experiment shows that our X-species is neutral the last process applies to our case. It is then efficiently cooled by the carrier gas (see Sect. 4.1) and relaxes to its ground state, X. Finally, upon absorption of a visible photon (over the range 580–820 nm), the X-radical suffers a new fragmentation and the C_2-molecule is ejected, very selectively excited in the level $d^3\Pi_g, v' = 3$. This sequence of fragmentation processes is described in Fig. 7.

Table 1. Frequencies (in cm^{-1}) of the vibrational modes of the unknown X-radical taken from the origin at 12,134 cm^{-1} together with those of neutral perylene and its cation, when these latter match the X frequencies, within 50 cm^{-1}. References for the measurements are: (a) states of the neutral (S_0 and S_1) by Fourman et al. (1985), Wittmeyer and Topp (1993) (jet), infrared active modes by Szczepanski et al. (1993) (Ar matrix), (b) ground electronic state of the cation (D_0) by Joblin et al. (1995) (Ne matrix), Negri and Zgierski (1994) (theory), infrared active modes by Szczepanski et al. (1993) and (c) present work (jet).

Neutral (a)			Cation (b)			X (c)
S_0	S_1	IR	D_0 (exp)	D_0 (th)	IR	
	95					94
350	353		357	373		315
585	628			624		604
	705		719	728	750	700
	900			871		910
		1132	1100	1129-1149	1128	1135
				1326	1318	
		1334		1365	1346	1340
	1370	1385	1390		1349	
		1613		1626		1670
		1765				1720
						2025
						2655
						2845
		3057-3065				3020
						3300
						3445

Table 2. We give here electronic fine structure line intervals taken from the origin of each vibronic band. See Figs. 5 and 6 for definition of $*$-bands and $\bullet$-bands.

ν (cm^{-1})	$\Delta\nu_1$	$\Delta\nu_2$	$\Delta\nu_3$	$\Delta\nu_4$	$\Delta\nu_5$	$\Delta\nu_6$	$\Delta\nu_7$	$\Delta\nu_8$
0 $*$	8.6		14.5	20.9	25.1	30.4	37.4	50.5
94 $\bullet$	8.6	12.2	13.7	19.9		30.1		
315 $*$	8.3		13.9	20.3	24.8	30.4	37.4	50.9
604 $\bullet$	7.7	11.9	–	–		–		
700 $\bullet$	8.1	–	–	18.6		31.3		
910 $*$	8.1		13.3	19.4	23.3	29.3	35.5	47.7
1135 $\bullet$	8.5	12.5	14.2	20.8		30.8		
1340 $\bullet$	8.7	12.3	14.1	20.6		30.7		
1670 $*$	8.3		13.6	20.3	24.6	30.0	37.0	49.6
1720 $\bullet$	8.6	12.4	14.0	20.1		30.0		
2655 $\bullet$	8.6	12.6	14.2	20.7		31.0		
2845 $\bullet$	8.7	12.6	14.7	21.0		31.0		
3020 $\bullet$	8.4	12.0	13.8	20.2		30.2		
3300 $*$	8.2		13.1	19.1	24.6	28.5	35.3	45.7
3445 $\bullet$	7.9	10.6	12.1	17.7		27.1		
3700 $*$	8.3		13.8	20.4	24.6	30.2	36.8	49.7
4210 $\bullet$	8.9	–	14.2	20.5		–		
4380 $\bullet$	8.8	12.3	14.2	20.6		30.4		
4530 $\bullet$	8.6	12.2	14.0	20.3		30.2		
4830 $*$	7.7		12.0	19.2	21.8	29.3	36.8	46.7
4890 $*$	8.2		13.3	19.6	23.7	29.1	35.5	47.8

5. Astrophysical relevance

5.1. The fate of perylene in the interstellar medium

The fragmentation process we observed in perylene may in fact exist in the ISM.

As we have seen, the jet produces cold, gas-phase molecules as in the ISM. Nevertheless, the photon excitation events occuring in our experiment bear, at first sight, no relationship to what happens in space. We show below that, on the contrary, the final X-product of our experiment may indeed be the same than the one produced if perylene had been placed in the ISM.

PAHs of sizes comparable to that of perylene can be shown to absorb average photons of about 10 eV in the diffuse ISM (Léger et al. 1989a). The interstellar radiation field is nevertheless dramatically weaker than that of our excimer laser: perylene in conditions of the diffuse ISM would absorb a photon every year or so (Léger et al. 1989a). In the ISM, the sequence is:

$$C_{20}H_{12} + h\nu \rightarrow I^* \Rightarrow I \text{ or } C_{20}H_{12} + h\nu \rightarrow R^* \Rightarrow R$$
$$I + h\nu \rightarrow X^* \Rightarrow X \text{ or } R + h\nu \rightarrow X^* \Rightarrow X$$

where **relaxations ($\Rightarrow$) are radiative** and are completed after a few 0.1 s. In our experiment, it is as if perylene absorbed sequentially two 10 eV-photons separated by 80 ps (see Sect. 4.3). The X^*-radical produced by these absorptions has not enough internal energy (a few eV, see Sect. 4.3), however, to fragment (or ionize) and **relaxes via collisions** towards the same species X as in the ISM. The X-fragment may not be an abundant species of the ISM because it easily dissociates to yield C_2. Photofragmentation of small PAHs may thus be an efficient formation mechanism of C_2 in the ISM. This could occur in irradiated regions, where small PAHs are produced by photodissociation or shock processing (Giard et al. 1992, Schmidt and Witt 1991). Some interesting environments are also objects like the RCB star V854, where at minimum brightness C_2 Swan bands have been observed with emission bands associated to DIBs (Rao and Lambert, 1993a and b).

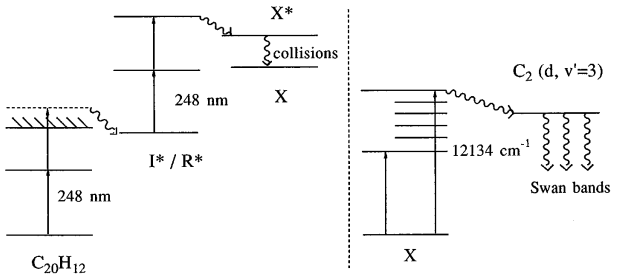

Fig. 7. Fragmentation sequence occuring in our experiment. Perylene sequentially absorbs 4 photons at 248 nm or equivalently two 10 eV-photons (see Sect. 4.2). After the first 10 eV-absorption an excited radical R^* or ion I^* is formed. It then absorbs 10 eV to yield another excited radical, X^*. This latter is cooled by collisions with the carrier gas and yields the X-species. Finally X absorbs a visible photon and dissociates, producing C_2 very selectively excited in the $(d^3\Pi_g, v' = 3)$ state. The fluorescence we observe emanates from the $(d, v' = 3) \rightarrow (a, v"$ =1 to 7)-transition (known as Swan bands).

Our experimental results illustrate the fragility of small PAHs in the ISM as had been pointed out earlier from statistical arguments (Léger et al. 1989b, Jochims et al. 1994). But it is not unlikely that some PAH photofragments may be more stable than their parent.

5.2. Implications for the DIBs

The X-radical observed in this experimental work cannot be a DIB carrier because it would be easily dissociated by visible photons in the ISM. Some conclusions relevant for DIBs can however be drawn from our results.

First, the absorption spectrum of a PAH radical at 0.1 cm^{-1} resolution has shown a high electronic multiplicity, which may be a general characteristics of large PAH radicals. The width of each set of bands is ~ 50 cm^{-1}, which is similar to the widths of the broadest DIBs. We can reasonably expect other derivatives of PAH molecules to possess similar spectral features. Moreover, the pattern of this fine structure depends highly upon the specific electronic properties of the molecular species, and therefore it is natural that many different patterns exist.

It seems of great importance now to search for the physical meaning of DIB profiles. Indeed, if we can understand which phenomenon broadens the bands (rotational, vibrational, electronic, intramolecular couplings...), we can draw conclusions on the carrier of these unidentified features. That is why many recent observational studies are conducted, with high-resolution

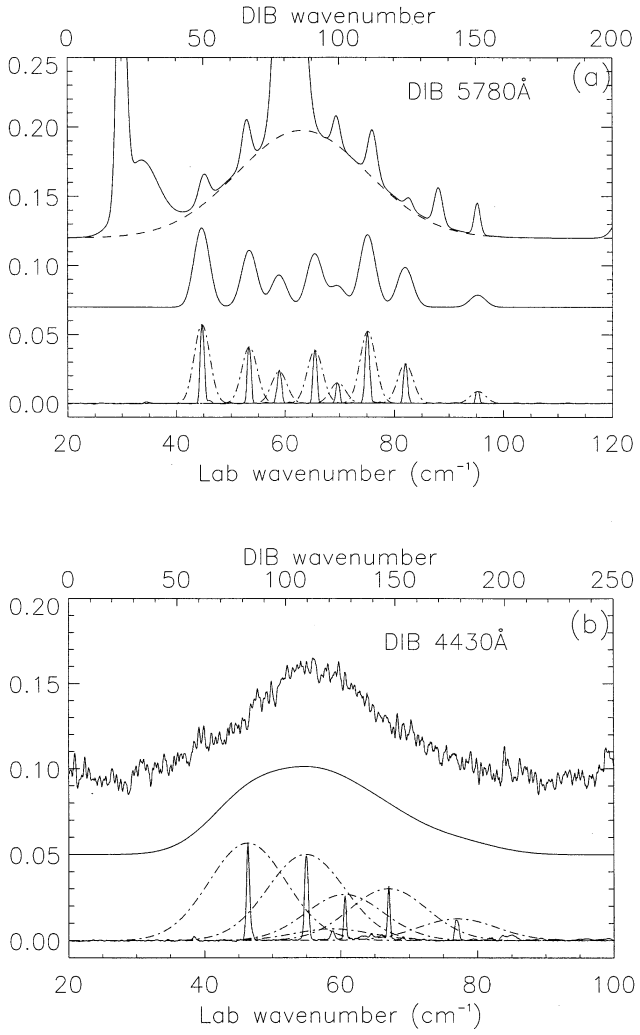

Fig. 8. a Comparison of a portion of the laboratory excitation spectrum showing a $*$-band convoluted with a 3 cm^{-1} FWHM gaussian, and a representative interstellar spectrum in the region of the 5780 Å DIB. Note that the scales differ by a factor of 2 in extension. **b** Similar comparison showing a •-band convoluted with a 13 cm^{-1} FWHM gaussian and a recording of the 4430 Å DIB towards HD 210839 (Moutou et al., not published). Note that the scales differ by a factor of 2.5.

spectroscopy (Sarre et al., 1995, Ehrenfreund and Foing, 1996, and Jenniskens et al., 1996). These observations are made usually on strong and narrow DIBs, such as 5797, 6613, 5850 Å... They reveal that profiles are rotational for these narrow DIBs, with 2 or 3 components: P, R and sometimes Q branches. For broad DIBs, no high-resolution spectrum exists and nothing is known about their broadening mechanism.

We wish to propose here a mechanism that may explain some patterns and profiles. Each individual line in the excitation spectrum of X (Fig. 6) is a rotational contour of a large molecular radical with a very low rotational temperature (a few K typically). In the ISM, it is very likely that such radicals have a much higher T_{rot}, at least equal to the gas temperature (30–100 K) (Rouan et al. 1992). Therefore, the narrow lines are broadened and may overlap. We have studied this broadening in the case of perylene, by using the same code as presented in section 4.1. Then we simulated the rotational contour by a gaussian profile, because it seems the best approximation to the spectra found in Cossart-Magos and Leach (1990) for coronene, showing weak wings. We evaluate the relationship between T_{rot} and the global rotational width FWHM $\delta\nu_{rot}$ for low temperatures, and extrapolate to higher temperatures where the computation is no more possible. The dependence is the following: $\delta\nu_{rot} \sim 0.5\sqrt{T_{rot}}$, in good agreement with the results of Cossart-Magos and Leach (1990). Fig. 8 shows some tentative broadenings for both types of bands (• and $*$), and the comparison of the resulting profile with some DIBs which have been selected for their shape regardless of their wavelengths. The spectrum of the X-species in the region of the origin band has been convolved with a $\delta\nu_{rot}$ = 3 cm^{-1} gaussian and the result is displayed in panel 8a along with the DIB survey spectrum near 5780 Å (Jenniskens and Désert 1994). Although the frequency scales differ, a striking similarity appears when the sequence of small peaks on both sides of the main DIB are considered. Indeed these peaks were found to be decorrelated in intensity from the main 5780 Å feature and its pedestal (dotted line in the figure), but correlated together (Krelowski and Sneden 1995). The fine structure spacings being molecule-dependent, the appropriate value of about 15 cm^{-1} could occur in the proper radical carrier. On the other hand, similar sequences of peaks, with different spacings, have been recognized throughout the DIB spectrum, in particular 11 cm^{-1} intervals around 6320 Å and 35 cm^{-1} around 6800 Å (Herbig and Leka, 1991).

In panel 8b the spectrum of the vibronic sequence at 94 cm^{-1} from the origin is convolved with a $\delta\nu_{rot}$ = 12 cm^{-1} gaussian. The unstructured resulting profile can be interestingly compared with that of the 4430 Å famous DIB, although the latter is 2.5 times broader. Other DIBs exhibiting 25 cm^{-1} width and regular shape can be found in the survey (like the 7930 Å for instance).

The rotational temperature of the DIB carrier required in such an interpretation, is T_{rot} = 40 K for case (a) and T_{rot} = 680 K for case (b), if this carrier would be of the size of perylene. The first value is perfectly reasonable for the diffuse ISM, and the second would invoke a heating mechanism like the "rocket" effect (Rouan et a., 1992) to be at work. These values would have to be corrected according to the size of the molecular carrier.

6. Conclusions

We have reported first results on LIF spectroscopy of jet-cooled species with the aim of identifying DIB carriers.u hey show that our experimental set-up produces cold, gas-phase and isolated ions or radicals and thus represents the best simulation to date of interstellar conditions. This technique relies on the detection of fluorescence photons. It is encouraged by the fact that recent work points out that fluorescent species could be the carriers of, at least, some DIBs. LIF spectroscopy appears thus a powerful tool to assert specific DIB assignments.

The fluorescence of a PAH cation, perylene, has recently been observed in condensed phase (rare-gas matrix) motivating us to study perylene. We failed to reproduce the matrix results. The reason may be related either to the species formed, or to the nature and/or efficiency of its luminescence. In spite of this, we recorded the absorption spectrum of a large perylene fragment, detected from the fluorescence of the photo-ejected C_2-molecule in its Swan bands.

Although this large radical has a near-infrared/visible absorption spectrum showing no coincidence with any DIB and is far too unstable to stand in the interstellar radiation field, this study leads to interesting avenues for the future of the DIB carriers searching game. It shows that, not only cations (which have long been suggested and more thoroughly studied in condensed phase), but also large PAH neutral radicals can be good candidates for DIB carrier identification.

Our results also illustrate the behaviour of PAHs in the interstellar medium: we observed a process in which perylene sequentially fragments while absorbing photons in a scheme similar to interstellar conditions to finally form the C_2-molecule. Other processes involving perylene or another PAH may however lead to a stable fragment possibly being a DIB carrier. Moreover, the spectral pattern we found in the present case may be common to many other PAH radicals, especially the electronic fine structure of the vibronic bands. This sheds new light on the DIB problem, in that we can interpret some broad DIBs or sequences of narrow DIBs as rotationally broadened electronic bands. Rotational temperatures of a few tens of K are sufficient to reproduce some common DIB series. With higher temperatures (a few 100 K) the fine structure is smeared out and a quasi-gaussian profile results, close to that of some broad DIBs.

Extension of this kind of studies to other DIB carrier candidates is presently in progress. The use of a mass spectrometer will allow to look specifically at cationaic species.

References

Birks, J., 1970, *Photophysics of aromatic molecules*, Wiley Interscience ed.

Birss, F.W., Ramsay, D.A., 1984, Comput. Phys. Commun., 38, 83

Bréchignac, P., De Benedictis, S., Nguyen Dai Hung & Halberstadt, N., 1986, Revue Phys. Appl., 21, 735

Clar, E., 1964, *"Polycyclic Hydrocarbons"*, Academic Press

Cossart-Magos,C. and Leach, S., 1990, A&A, 233, 559

Crawford, M.K., Tielens, A.G.G.M., Allamandola, L.J., 1985, ApJ, 293, L45

Danylewych, L.L. and Nicholls, R.W., 1974, Proc. R. Soc. Lond. A., 339, 197–222

Dhumwad, R.K., Pathwardhan, A.B., Kulkarni, V.T., Savadatti, M.I., 1981, J. of Molec. Spectr., 85, 177

Ehrenfreund, P., d'Hendecourt, L., Verstraete, L., Léger, A., Schmidt, W., Défourneau, D., 1992a, A&A, 259, 257

Ehrenfreund, P., d'Hendecourt, L., Joblin, C., Léger, A., 1992b, A&A, 266, 429

Ehrenfreund, P., Foing, B., 1996, A&A, 307, L25

Fillaux, F., 1985, Chem. Phys. Lett., 114 (4), 384

Flinckinger, G.C., Wdowiak, T.J. Gomez, P.L., 1991, ApJ, 380, L43

Foing, B. and Ehrenfreund, P., 1994, Nature, 369,296

Fourman, B., Jouvet, C., Tramer, A., Le Bars, J.M. Millie, Ph., 1985, Chem. Phys., 92, 25

Giard, M., Bernard, J.P. and Dennefeld, M., 1992, A&A, 264, 610.

Gotkis, Y., Oleinikova, M., Naor, M. and Lifshitz, C., 1993, J. Phys. Chem., 97, 12282

Herbig, G.H. and Leka, K.D., 1991, ApJ, 382, 193

Herbig, G.H., 1995, Ann. Rev. of A&A, 33

Jenniskens, P., Désert, F.X., 1994, A&A Suppl. Ser., 106, 39

Jenniskens, P., Porceddu, I., Benvenuti, P., and Désert, F.X., 1996, A&A, in press

Joblin, C., Léger, A., Martin, P., 1992, ApJ, 393, L79

Joblin, C., Salama, F., Allamandola, L., 1995, in *"The Diffuse Interstellar Bands"*, Tielens & Snow eds.

Joblin, C., Salama, F., Allamandola, L., 1995, J. Chem Phys., 102 (24), 9743

Jochims, H.W., Rühl, E., Baumgärtel, H., Tobita, S., Leach, S., 1994, ApJ, 420, 307

Krelowski, J. and Sneden, C., 1995, in *"The Diffuse Interstellar Bands"*, Tielens & Snow eds.

Kurtz, J., 1992, A&A, 255, L1

Leach, S., 1987, in *"PAHs and Astrophysics"*, Léger, d'Hendecourt & Boccara, Reidel Publishing Company

Léger, A., d'Hendecourt, L., 1985, A&A, 146, 81

Léger, A., d'Hendecourt, L., Défourneau, D., 1989a, A&A, 216, 148

Léger, A., Boissel, P., Désert, F.X., d'Hendecourt, L., 1989b, A&A, 213, 351

Léger, A., 1994, in *"The Diffuse Interstellar Bands"*, Tielens & Snow eds.

Léger, A., d'Hendecourt, L., Défourneau, D., 1995, A&A, 293, L53

Ling, Y. and Lifshitz, 1995, J. Phys. Chem, 99, 11074

Moreels, G., Clairemidi, J., Hermine, P., Bréchignac, P., Rousselot, P., 1994, A&A, 282, 643

Naulin, C., Costes, M. and Dorthe, G., 1988, Chem. Phys. Lett., 143, 496

Parisel, O., Berthier, G., Ellinger, Y., 1992, A&A, 266, L1

Rao, N.K., Lambert, D.L., 1993a, Astr. Journal, 105 (5), 1915.

Rao, N.K., Lambert, D.L., 1993b, M.N.R.A.S. 263, L27

Rouan, D., Léger, A., Omont, A., Giard, M., 1992, A&A, 253, 498

Salama, F., Allamandola, L.J., 1992a, ApJ, 395, 301

Salama, F., Allamandola, L.J., 1992b, Nature, 358, 42

Salama, F., Allamandola, L.J., 1993, J. Ch. Soc. Faraday Tr., 89(13), 2277

Sarre, P.J., Miles, J.R., Kerr, T.H., Hibbins, R.E., Fossey, S.J., Somerville, W.B., 1995, MNRAS, 277, L41

Scarrott, S.M., Watkin, S., Miles, J.R., Sarre, P.J., 1992, MNRAS, 255, 11P

Schmidt, G.D. and Witt, A.N., 1991, ApJ, 383, 698.

Schwartz, S.A., Topp, M.R., 1984, Chem. Phys., 86, 245

Smith, R.S., Anselment, M., DiMauro, L.F., Frye, J.M., Sears, T.J., 1987, J. Chem. Phys., 87 (8), 4435

Smith, R.S., Anselment, M., DiMauro, L.F., Frye, J.M., Sears, T.J., 1988, J. Chem. Phys., 89 (4), 2591

Szczepanski, J., Chapo, C., Vala, M., 1993, Chem. Phys. Lett., 205, 434

Wittmeyer, S.A., Topp, M.R., 1993, J. Phys. Chem., 97, 8718

van der Zwet, G.P., Allamandola, L.J., 1985, A&A, 146, 76